

Phase diagram of an extended Kondo lattice model for manganites: the Schwinger-boson mean-field approach

R. Y. Gu, Z. D. Wang, Shun-Qing Shen

Department of Physics, The University of Hong Kong, Pokfulam Road, Hong Kong

D. Y. Xing

National Laboratory of Solid State Microstructures and Department of Physics, Nanjing University, Nanjing 210093, China
(January 27, 2017)

We investigate the phase diagram of an extended Kondo lattice model for doped manganese oxides in the presence of strong but finite Hund's coupling and on-site Coulomb interaction. By means of the Schwinger-boson mean-field approach, it is found that, besides magnetic ordering, there will be non-uniform charge distributions, such as charge ordering and phase separation, if the interaction between electrons prevails over the hybridization. Which of the charge ordering and phase separation appears is determined by a competition between effective repulsive and attractive interactions due to virtual processes of electron hopping. Calculated results show that strong electron correlations caused by the on-site Coulomb interaction as well as the finite Hund's coupling play an important role in the magnetic ordering and charge distribution at low temperatures.

I. INTRODUCTION

The doped manganese oxides with perovskite structure, $R_{1-x}A_x\text{MnO}_3$ ($R=\text{La, Pr, Nd}$; and $A=\text{Sr, Ca, Ba, Pb}$), have recently attracted much attention due to the observation of colossal magnetoresistance (CMR).¹⁻⁴ Theories based on the double exchange (DE) model,⁵⁻⁷ in which the exchange of electrons between neighboring manganese ions with a strong Hund's coupling drives spins of on-site electrons to align parallelly, have been developed for a long time and can qualitatively elucidate the relation of transport and magnetism in the doping range of $0.2 < x < 0.45$. However, recent systematic experimental studies revealed rich phase diagrams, which are difficult to be understood by the DE model alone. For instance, the system is actually insulating in the half-doping case ($x = 0.5$) at low temperature; but a metallic ferromagnetic (FM) state would be expected according to the DE model, for the DE hopping reaches its maximum and the effective FM interaction becomes strongest at this doping. Furthermore, for $x = 0.5$, a charge ordering characterized by an alternating Mn^{3+} and Mn^{4+} -ion arrangement in the real space was observed to be superimposed on the antiferromagnetic (AF) ordering.^{8,9} This charge ordering is sensitive to an applied magnetic field, and even melts under a moderate magnetic field. In the meantime, the resistance may decrease by several orders in magnitude,^{9,10} implying that there is a close relation between the charge ordering and the AF spin background.

Many efforts have been made to understand the phase diagram of a doped manganese oxide based on various models.¹¹⁻¹⁵ To explore the origin of the unique magnetotransport, many further theories on the basis of DE model have been proposed, such as Jahn-Teller displacement and electron-phonon interactions,^{16,17} spin-polaron formation,¹⁸ Anderson localization with diago-

nal and off-diagonal disorder,^{19,20} and the phase separation scenario.^{21,22} Importance of various interactions on the physical properties of the manganites is currently one of the lively-debating subjects. A comprehensive understanding of the magnetic and charge ordering states as well as their relations to the transport properties are highly desirable.

In this paper, we investigate effects induced by strong but finite Hund's coupling J_H and on-site Coulomb interaction U . In the manganites, three t_{2g} electrons are almost localized and form an $S = 3/2$ spin state according to the Hund's rule, while electrons in e_g orbit evolve a conduction band. In the conventional DE model J_H is usually regarded to be infinite and U is neglected, so that there exist only single-occupied state with spin $S + 1/2$ and empty state with spin S . In this limit, since neither $S - 1/2$ state nor double occupancy of e_g electrons on the same site is allowed, the effects induced by two kinds of virtual processes, that an electron hops to a empty site with its spin antiparallel to the core spin on the site and that an electron hops to a singly-occupied site, are completely eliminated. In this work we will show that the effects due to the two kinds of virtual processes are important to account for the observed phase diagrams. On one hand, the two kinds of virtual processes can produce an AF superexchange coupling between the neighboring localized spins, with coupling strength being $t^2/(2J_H)$ and $t^2/(J_H + U)$, respectively, where t is the hopping integral of the e_g electron. The AF coupling induced by the virtual processes is usually much stronger than the direct AF superexchange coupling between neighboring localized spins. On the other hand, the virtual process of producing a single-occupied state with spin $S - 1/2$ can lead to a repulsive interaction between conduction electrons, while the virtual process of producing a double occupancy can result in an attractive one, as will be shown in Sec. IIA. The two types of interactions between

electrons can produce non-uniform charge distributions, such as charge ordering and electronic phase separation, provided that the interactions prevail over the hybridization effects of electrons. Which of charge ordering and phase separation appears is determined by a competition at different doping between two types of interactions, for the repulsive interaction is favorable to the charge ordering while the attractive interaction may cause the phase separation.

In Sec. II, starting from an extended Kondo lattice model, we have an effective projected Hamiltonian in the case of strong but finite J_H and U . The repulsive and attractive interactions, which are associated with magnetic ordering and non-uniform charge distributions, are obtained. A Schwinger-boson mean-field theory is developed to establish the phase diagram at low temperatures. In Sec. III we focus attention on the case of $x = 1/2$. The possibility that the FM, AF or canted ferromagnetic (CF) order appears, as well as that the Wigner lattice or phase separation appears, is discussed. In Sec. IV numerical results for phase diagram are presented. In the large J_H case, the hybridization effect is dominant and there exists metallic ferromagnetism, which accords with the DE model. As the repulsive interaction due to finite J_H effects is relatively strong, the charge ordering will be formed at half doping in the AF background. On the other hand, the phase separation may arise when the attractive interaction due to finite U becomes dominant.

II. GENERAL FORMALISM

A. Effective projected Hamiltonian

The electronic model Hamiltonian for doped manganese oxides we considered presently is given by

$$H = -t \sum_{(ij),\sigma} c_{i\sigma}^\dagger c_{j\sigma} + U \sum_i n_{i\uparrow} n_{i\downarrow} - J_H \sum_{i\sigma\sigma'} c_{i\sigma}^\dagger \mathbf{S}_i \cdot \boldsymbol{\sigma}_{\sigma\sigma'} c_{i\sigma'} + J_{AF} \sum_{(ij)} \mathbf{S}_i \cdot \mathbf{S}_j. \quad (1)$$

Here $c_{i\sigma}$ ($c_{i\sigma}^\dagger$) is the annihilation (creation) operator for conduction electrons at site i with spin σ , $n_{i\sigma} = c_{i\sigma}^\dagger c_{i\sigma}$ is the particle number operator, \mathbf{S}_i is the total spin operator of the localized electrons at site i with $S = 3/2$, and $\boldsymbol{\sigma}$ is the Pauli matrix. In the manganites the Hund's coupling constant J_H and the on-site Coulomb interaction U are much greater than the hopping integral t as well as the direct AF superexchange coupling J_{AF} . On a given site, an itinerant electron constrained by the strong Hund's coupling has its spin parallel to the core spin, forming a spin $S+1/2$ state. The singly-occupied state for the itinerant electron with spin antiparallel to the core spin and the doubly-occupied state are almost forbidden, making it appropriate to utilize the projective perturbation technique to investigate Hamiltonian (1). The effects of finite

J_H and U can be regarded as a perturbation correction to the large J_H and U limit where there are only the empty and single occupancy with $S+1/2$ state. Up to the second-order perturbation, an effective Hamiltonian for Eq. (1) can be derived as²³

$$H_{eff} = -t \sum_{(ij),\sigma} \bar{c}_{i\sigma}^\dagger \bar{c}_{j\sigma} + J_{AF} \sum_{(ij)} \bar{\mathbf{S}}_i \cdot \bar{\mathbf{S}}_j + J_1 \sum_{(ij)} (\mathbf{S}_i \cdot \tilde{\mathbf{S}}_j - S\tilde{S}) P_{ih} P_{js}^\dagger + J_2 \sum_{(ij)} (\tilde{\mathbf{S}}_i \cdot \tilde{\mathbf{S}}_j - \tilde{S}^2) P_{is}^\dagger P_{js}^\dagger. \quad (2)$$

Here $\tilde{\mathbf{S}}_i$ is the spin operator with $\tilde{S} = S+1/2$. P_{ih} and P_{is}^\dagger are the projection operators for empty state with spin \mathbf{S}_i and single occupancy with spin $\tilde{\mathbf{S}}_i$, respectively. $\bar{\mathbf{S}}_i = \mathbf{S}_i P_{ih} + S\tilde{\mathbf{S}}_i P_{is}^\dagger / \tilde{S}$. $\bar{c}_{i\sigma} = P_i c_{i\sigma} P_i$ and $\bar{c}_{i\sigma}^\dagger = P_i c_{i\sigma}^\dagger P_i$ are projected electron operators, where $P_i = P_{ih} + P_{is}^\dagger$, projects onto the space of non-doubly-occupied site. The last two terms in Eq. (2) are the second-order perturbation corrections where $J_1 = t^2 / (2J_H \tilde{S}^3)$ and $J_2 = t^2 / [(J_H S + U) \tilde{S}^2]$, respectively, stemming from different virtual processes (a) and (b). In virtual process (a), an electron first hops from a site to one of the nearest-neighbor empty sites to form a spin $S-1/2$ state and then hops backward; while in virtual process (b), an electron first hops to a single-occupied site, where there has been an electron with opposite spin, and then hops backward. Owing to $J_1 > 0$ and $J_2 > 0$, both virtual processes favor the AF arrangement of the core spins and enhance greatly the AF coupling between the neighboring spins. Whether non-uniform charge distributions can appear is determined by a competition between electronic hybridization and interactions of electrons with one another. The hybridization, the overlap of electron wavefunctions centred on different sites, is a quantum-mechanical effect that allows electrons to hop from one atom to another, thus tending to spread the electronic density uniformly through the system. In contrast, the interactions of electrons in the system tend to promote non-uniform charge distributions.²⁴ The addition of the last two terms in Eq. (2), arising from the finite J_H and U effects, enhances greatly the interaction side in the competition and thus favors the occurrence of the non-uniform charge distributions. On the other hand, since the values of $J_1(\mathbf{S}_i \cdot \tilde{\mathbf{S}}_j - S\tilde{S})$ and $J_2(\tilde{\mathbf{S}}_i \cdot \tilde{\mathbf{S}}_j - \tilde{S}^2)$ are always non-positive, it is clear that the two terms represent the repulsive and attractive interactions between conduction electrons on neighboring sites, respectively. The competition between them will lead to different non-uniform charge distributions, the charge-ordered state and the phase separation.

B. Schwinger boson representation

A projected electron operator may be regarded as a combination of the operator f for a spinless charge fermion and that for a neutral boson with spin $\tilde{S} = S + 1/2$, i.e., $\bar{c}_{i\sigma} = f_i b_{i\sigma} / \sqrt{2\tilde{S}}$, where $b_{i\sigma}$ is the Schwinger boson operator.²⁵ In the Schwinger boson representation, the spin \mathbf{S}'_i ($\mathbf{S}'_i = \mathbf{S}_i$ or $\tilde{\mathbf{S}}_i$) can be expressed as $\mathbf{S}'_i = \frac{1}{2} \sum_{\sigma\sigma'} b_{i\sigma}^\dagger \boldsymbol{\sigma}_{\sigma\sigma'} b_{i\sigma'}$, with constraint $\sum_{\sigma} b_{i\sigma}^\dagger b_{i\sigma} = 2S'$ ($S' = S$ or \tilde{S}). This constraint can also be written as $\sum_{\sigma} b_{i\sigma}^\dagger b_{i\sigma} = 2S + n_i$, where $n_i = f_i^\dagger f_i$ is the particle number operator of fermions. The projection operators can be replaced by $P_{ih} = 1 - n_i$ and $P_{is}^\dagger = n_i$. Then, by using the identity $\mathbf{S}'_i \cdot \mathbf{S}'_j = -\frac{1}{2} A_{ij}^\dagger A_{ij} + S'_i S'_j$ with $A_{ij} = \frac{1}{2}(b_{i\uparrow} b_{j\downarrow} - b_{i\downarrow} b_{j\uparrow})$, the effective Hamiltonian is reduced to

$$H = J_{AF} S^2 - \tilde{t} \sum_{ij} f_i^\dagger f_j F_{ij} - \frac{1}{2} A_{ij}^\dagger A_{ij} [J_{AF} + \tilde{J}_1(1 - n_i)n_j + \tilde{J}_2 n_i n_j], \quad (3)$$

where $F_{ij} = \sum_{\sigma} b_{i\sigma}^\dagger b_{j\sigma}$, $\tilde{t} = t/(2\tilde{S})$, $\tilde{J}_1 = J_1 - J_{AF}/\tilde{S}$ and $\tilde{J}_2 = J_2 - J_{AF}/\tilde{S} + J_{AF}/4\tilde{S}^2$. The difference between \tilde{J}_n and J_n ($n=1$ and 2) is caused by the finite S effect, and would disappear in the large spin limit.

C. Mean-field approximation

We now make a Hartree-Fock mean-field approximation by decoupling various terms in Eq.(3). As an example, we have

$$\begin{aligned} A_{ij}^\dagger A_{ij} n_i n_j &\rightarrow A_{ij}^\dagger \langle A_{ij} \rangle \langle n_i \rangle \langle n_j \rangle \\ &+ \langle A_{ij}^\dagger \rangle A_{ij} \langle n_i \rangle \langle n_j \rangle \\ &+ \langle A_{ij}^\dagger \rangle \langle A_{ij} \rangle n_i \langle n_j \rangle \\ &+ \langle A_{ij}^\dagger \rangle \langle A_{ij} \rangle \langle n_i \rangle n_j \\ &- 3 \langle A_{ij}^\dagger \rangle \langle A_{ij} \rangle \langle n_i \rangle \langle n_j \rangle . \end{aligned}$$

For the fermions, we have $\langle n_i \rangle = 1 - x$ in a uniform density state. In the presence of the charge ordering at $x = 1/2$, the lattice can be divided into two sublattices $X = A$ and B , and $\langle n_i \rangle = N_X = 1 - x + \alpha\delta$ where $\alpha = 1$ or -1 for $i \in A$ or B , and δ ($0 \leq \delta \leq 1 - x$) is the charge ordering parameter. The uniform state can be regarded as a special case of $\delta = 0$. As in Ref.^{26,15}, the FM and AF order parameters can be respectively written as

$$\begin{aligned} \langle F_{ij} \rangle &= F, \\ \langle A_{ij} \rangle &= (-1)^{r_i} A, \end{aligned}$$

where r_i depends on the position of site i , being an odd number in one sublattice and an even number in the other

sublattice. The average value of $\langle f_i^\dagger f_j \rangle$ is assumed to be a constant K . Under the Hartree-Fock mean-field approximation, Hamiltonian (3) is reduced to

$$H_{MF} = E_0 + H_{Bose} + H_{Fermi} \quad (4)$$

with

$$\begin{aligned} E_0 &= NZ\tilde{t}KF + NZJ_{AF}S^2 - N\Lambda 2S \\ &+ \frac{1}{2}NZ A^2 \{J_{AF} + 2(1-x)\tilde{J}_1 \\ &+ 3[(1-x)^2 - \delta^2](\tilde{J}_2 - \tilde{J}_1)\} \\ H_{Bose} &= \sum_{(ij)} \frac{-\tilde{J}}{2} (-1)^{r_i} A(A_{ij}^\dagger + A_{ij}) \\ &+ \Lambda \sum_{i\sigma} b_{i\sigma}^\dagger b_{i\sigma} - \tilde{t}K \sum_{(ij)\sigma} b_{i\sigma}^\dagger b_{j\sigma}, \\ H_{Fermi} &= -\tilde{t}F \sum_{(ij)} f_i^\dagger f_j - (\Lambda + \mu) \sum_i n_i \\ &- \frac{1}{2} A^2 Z \sum_i [2(\tilde{J}_2 - \tilde{J}_1)N_{\bar{X}} + \tilde{J}_1] n_i. \end{aligned}$$

Here $\tilde{J} = J_{AF} + (\tilde{J}_2 - \tilde{J}_1)[(1-x)^2 - \delta^2] + \tilde{J}_1(1-x)$ is the effective AF coupling constant, N is the number of lattice sites, Z is the coordinate number of the lattice, and $N_{\bar{X}} = N_B$ (N_A) for $i \in A$ (B). $\Lambda = \langle \Lambda_i \rangle$ with Λ_i being the Lagrange multiplier introduced at site i to enforce the local constraint $\sum_{\sigma} b_{i\sigma}^\dagger b_{i\sigma} = 2S + n_i$,²⁵ and μ is the chemical potential of fermions which is determined by the total conduction electron number. After diagonalizing H_{Bose} and H_{Fermi} , we have

$$H_{Bose} = \sum_{\mathbf{k}\sigma} E_{\mathbf{k}} \beta_{\mathbf{k}\sigma}^\dagger \beta_{\mathbf{k}\sigma} + \sum_{\mathbf{k}} (E_{\mathbf{k}} - \Lambda),$$

and

$$H_{Fermi} = \sum_{\mathbf{k}} (\varepsilon_{\mathbf{k}} - \tilde{\mu}) \psi_{\mathbf{k}}^\dagger \psi_{\mathbf{k}},$$

with boson and fermion dispersions as

$$E_{\mathbf{k}} = \sqrt{\Lambda^2 - (Z A \tilde{\gamma}_{\mathbf{k}})^2 - Z \tilde{t} K \gamma_{\mathbf{k}}},$$

and

$$\varepsilon_{\mathbf{k}} = -\text{sgn}(\gamma_{\mathbf{k}}) Z \sqrt{A^4 (\tilde{J}_2 - \tilde{J}_1)^2 \delta^2 + \tilde{t}^2 F^2 \gamma_{\mathbf{k}}^2},$$

respectively. Here $\gamma_{\mathbf{k}} = Z^{-1} \sum_{\boldsymbol{\eta}} e^{i\mathbf{k}\cdot\boldsymbol{\eta}}$ with $\boldsymbol{\eta}$ the vector of the nearest neighbors of each site, and the shifted chemical potential is given by

$$\tilde{\mu} = \mu + \Lambda + \frac{1}{2} Z A^2 [\tilde{J}_1 + 2(\tilde{J}_2 - \tilde{J}_1)(1-x)].$$

From the fermion spectrum, it is found that the energy band of fermions is divided into two separated branches, between which there is an energy gap provided $\delta \neq 0$ and $\tilde{J}_2 \neq \tilde{J}_1$. Thus, in the half-doping case ($x = 1/2$) at zero temperature, the lower branch ($\gamma_{\mathbf{k}} > 0$) is fully occupied by fermions while the upper one ($\gamma_{\mathbf{k}} < 0$) is empty.

III. CHARGE ORDERING AND PHASE SEPARATION

Now we come to discuss the magnetic ordering and non-uniform charge distributions at $x = 0.5$. First let us write down the mean-field equations. When the magnetic ordering arises, the Schwinger bosons should condensate to the lowest energy state. From $E_{\mathbf{k}=0} = 0$, we have

$$\Lambda = Z\sqrt{\tilde{t}^2 K^2 + A^2 \tilde{J}^2}.$$

Using the spectra of quasi-fermions and bosons, we obtain a set of self-consistent equations at zero temperature:

$$K = \frac{1}{2N} \sum_{\mathbf{k}} \frac{\tilde{t}F\gamma_{\mathbf{k}}^2}{\sqrt{(\tilde{J}_1 - \tilde{J}_2)^2 A^4 \delta^2 + \tilde{t}^2 F^2 \gamma_{\mathbf{k}}^2}}, \quad (5a)$$

$$F = \frac{\tilde{t}K(2S + 2 - x)}{\sqrt{\tilde{t}^2 K^2 + A^2 \tilde{J}^2}} - \frac{1}{N} \sum_{\mathbf{k}} \frac{\tilde{t}K}{\sqrt{\tilde{t}^2 K^2 + A^2 \tilde{J}^2 (1 - \gamma_{\mathbf{k}}^2)}}, \quad (5b)$$

$$A = \frac{A\tilde{J}(2S + 2 - x)}{\sqrt{\tilde{t}^2 K^2 + A^2 \tilde{J}^2}} - \frac{1}{N} \sum_{\mathbf{k}} \frac{A\tilde{J}(1 - \gamma_{\mathbf{k}}^2)}{\sqrt{\tilde{t}^2 K^2 + A^2 \tilde{J}^2 (1 - \gamma_{\mathbf{k}}^2)}}, \quad (5c)$$

$$\delta = \frac{1}{2N} \sum_{\mathbf{k}} \frac{(\tilde{J}_1 - \tilde{J}_2)A^2 \delta}{\sqrt{(\tilde{J}_1 - \tilde{J}_2)^2 A^4 \delta^2 + \tilde{t}^2 F^2 \gamma_{\mathbf{k}}^2}}. \quad (5d)$$

From Eq. (5d), it follows that the charge ordering may appear ($\delta \neq 0$) only when $\tilde{J}_1 > \tilde{J}_2$, otherwise there exists only a trivial solution of $\delta = 0$. Physically, the effective interaction between electrons is repulsive for $\tilde{J}_1 - \tilde{J}_2 > 0$, which is responsible for the formation of the charge ordering. There are two types of possible ordering states: the pure magnetic ordering phase without charge order and the charge ordering phase in which the charge and magnetic orders coexist. The former includes FM, AF, and CF phases; while the latter is the Wigner lattice ($\delta = 1/2$, $K = F = 0$, and $A = A_{max}$) or a combination of the charge ordering ($0 < \delta < 1/2$) and magnetic ordering ($A < A_{max}$, K and $F \neq 0$). Since the system under consideration is a three-dimensional (3D) simple-cubic lattice, for convenience, we introduce two parameters $\eta_1 = \tilde{t}^2 F^2 / [(\tilde{J}_1 - \tilde{J}_2)^2 A^4 \delta^2]$ ($0 \leq \eta_1 \leq \infty$) and $\eta_2 = -A^2 \tilde{J}^2 / (\tilde{t}^2 K^2 + A^2 \tilde{J}^2)$ ($-1 \leq \eta_2 \leq 0$) and define the following two 3D integrals:

$$C_i = \frac{1}{N} \sum_{\mathbf{k}} \frac{1}{\sqrt{1 + \eta_i \gamma_{\mathbf{k}}^2}},$$

$$D_i = \frac{1}{N} \sum_{\mathbf{k}} \frac{\gamma_{\mathbf{k}}^2}{\sqrt{1 + \eta_i \gamma_{\mathbf{k}}^2}}.$$

with $i = 1, 2$. Then the set of mean-field equations (5a)-(5d) can be rewritten as

$$K = \frac{1}{2} \sqrt{\eta_1} D_1, \quad (6a)$$

$$F = \sqrt{1 + \eta_2} (2S + 2 - x - C_2), \quad (6b)$$

$$A = \sqrt{-\eta_2} (2S + 2 - x - C_2 + D_2), \quad (6c)$$

$$\delta = \frac{1}{2} C_1. \quad (6d)$$

For the Wigner lattice ($\delta = 1/2$), from Eq. (6d), it follows $C_1 = 1$ and $\eta_1 = 0$, so that $K = 0$, $\eta_2 = -1$, and $F = 0$. In this case, A reaches its maximum $A_{max} \approx 2S + 0.597$, indicating a fully AF insulator in which all the electrons are localized in one sublattice. Another limiting case is that there is no charge ordering ($\delta = 0$), where there are two sets of solutions: (i) $K = F = 0$ and $A = A_{max}$, which is an AF state; and (ii) $\eta_1 = +\infty$, $K \neq 0$, and $F \neq 0$, which is a CF state for $0 < A < A_{max}$ or a FM state for $A = 0$. There is the lowest energy in the ground state. This ground state energy per site in the AF state [case (i)] is

$$E_g = -\tilde{J} A_{max}^2 / 2, \quad (7)$$

and that for case (ii) is given by

$$E_g = -\frac{(2S + 2 - x - C_2 - \eta_2 D_2) \tilde{t}}{6\sqrt{1 + \eta_2}} - \frac{\tilde{t}^2 \eta_2}{72\tilde{J}(1 + \eta_2)}, \quad (8)$$

which is a function of η_2 . For a CF state, the magnitude of η_2 is determined by minimizing E_g , i.e., $\partial E_g / \partial \eta_2 = 0$. $\eta_2 = 0$ corresponding to a FM state. It is found that a phase transition occurs from a CF state to a FM state when \tilde{J} decreases to $\tilde{t}/(12S + 9)$.

The uniform density phases discussed above may be unstable toward the phase separation, which will occur if $\partial \mu / \partial x \leq 0$. In our model, when the virtual process (b) is dominant over process (a), i.e., $\tilde{J}_2 > \tilde{J}_1$, the effective interaction between the e_g electrons on neighboring sites will be attractive. If such an attractive interaction is strong enough, the e_g electrons will tend to accumulate together to lower the total energy of the system. In this case, the electronic density is no longer uniform and the phase separation occurs between electron-rich and electron-poor regions. The chemical-potential judgment of phase separation is $\partial \mu / \partial x \leq 0$, equivalent to the energy judgment $\partial^2 E_g / \partial x^2 \leq 0$ due to $\mu = \partial E_g / \partial x$. The phase separation will appear when $\partial^2 E_g / \partial x^2 \leq 0$, where both η_2 and \tilde{J} in Eqs. (7) and (8) are functions of x .

IV. PHASE DIAGRAMS AND DISCUSSIONS

Mean-field equations (6a)-(6d) have been numerically solved and the phase diagrams at $x = 0.5$ are plotted in Figs. 1 and 2. To make the results comparable with

each other for different S , we have used reduced coupling constants $j_{af} = J_{AF}S^2$ and $j_h = J_H\tilde{S}$. Fig. 1 is the phase diagram of j_{af}/t and t/j_h in the large U limit with $S = 3/2$ and $S \rightarrow \infty$. In this case, $J_2 = 0$, and t/j_h indicates the ratio of the repulsive interaction due to virtue process (a) to the kinetic energy of the e_g electron. It is found that the system is in the FM state for small j_{af}/t and t/j_h , where either direct or indirect AF superexchange coupling is weak compared with the FM coupling due to the DE mechanism. With increasing j_{af}/t and t/j_h , the AF superexchange coupling between the neighboring localized spins is enhanced. As $\tilde{J} \geq \tilde{t}/(12S + 9)$, the CF state appears; meanwhile, a repulsive interaction between fermions is increased due to the increase of t/j_h . At this stage, there is a CF ordering but the charge ordering has not yet arisen, which is labeled as the CF1 state in Figs. 1 and 2. When t/j_h is increased beyond a threshold so that the repulsive potential between fermions dominates over the kinetic energy, the fermions begin to tend toward one sublattice and thus charge ordering emerges, which is called as the CF2 state. Finally, with further increase of t/j_h , δ increases gradually. At $\delta = 1/2$, all the e_g electrons are confined in one sublattice in the AF background, forming a Wigner lattice. It is found that the phase diagram for $S = 3/2$ is very similar to that for $S \rightarrow \infty$. The difference between them can be seen in the large j_{af}/t case, for the effective repulsive interaction is proportional to the factor $\tilde{J}_1 - \tilde{J}_2$ or $t/j_h - j_{af}/(2tS^2\tilde{S})$. For finite S , the increase of j_{af} will decrease this factor and so be unfavorable to the charge ordering. As a result, the quantum fluctuation of finite S leads to enlargements of the CF1 and CF2 regions.

For manganites, it is roughly estimated that $t \approx 0.15eV$, $j_h \approx 0.75eV$, $U \approx 10eV$, and $j_{af} \approx 8meV$,²⁷ so that $j_{af}/t \approx 0.05$ and $t/j_h \approx 0.2$. From Fig. 1, it follows that the repulsive interaction from virtual process (a) alone enables the e_g electrons to form the charge ordering. This indicates that this process plays an important role in determining the collective behavior of electrons. In actual doped manganites, there may also be other effects that favor charge ordered phase, which are not considered in the present paper, such as the direct nearest-neighbor Coulomb interactions.^{10,27,28} It is worth pointing out here whether the charge ordering occurs depends not only the ratio of t/j_h , but also the magnetic ordering of the system. In doped manganites, the amplitude for an electron to hop from one site to another is determined by the relative orientation between the core spins at the two sites, being greatest when the core spins are parallel and least when they are antiparallel. As a result, a FM state has the greatest hybridization and so tends to spread the electronic density uniformly through the system; while an AF state has the least hybridization and favors the charge ordering. This can account for the sensitivity of charge ordering with respect to an applied magnetic field that tends always to align the core spins.^{9,10} Besides, there is a difference between two types

of repulsive interactions mentioned above in the response to an applied magnetic field: with a decrease in the AF correlation, the superexchange electron-electron interaction is reduced, while the direct Coulomb interaction remains unchanged. Therefore, charge ordering caused by virtual process (a) is more easily affected by the magnetic field than that caused by the direct Coulomb interaction.

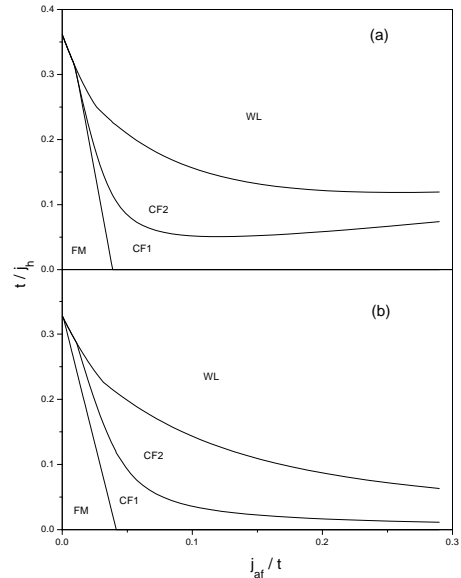


FIG. 1. Phase diagram of the extended Kondo lattice model with $U = \infty$ for (a) $S = 1.5$ and (b) $S \rightarrow \infty$. FM, CF1, and CF2 denote regimes of metallic ferromagnet, canted ferromagnet without and with charge ordering, respectively. WL stands for the Wigner lattice.

In Fig. 2, we present the phase diagram of $j_h/(j_h + U)$ and t/j_h . In the finite U case, $j_h/(j_h + U)$ describes the relative strength of the effective interaction due to virtual process (b) to that due to process (a). For small t/j_h , there is only a FM state, where the Hund's coupling is very strong, both virtual processes (a) and (b) are suppressed so that the hybridization effect and the DE ferromagnetism dominates over the system. With increasing t/j_h , both J_1 and J_2 become large and so the AF superexchange coupling due to virtue processes (a) and (b) is enhanced, leading to the CF1 state. As t/j_h is increased beyond a threshold, the charge ordering or phase separation may occur, depending on the compe-

tion between effective repulsive and attractive interactions. For $j_h < U$, $\tilde{J}_1 > \tilde{J}_2$, the net repulsive interaction favors the charge ordering. The opposite case is $\tilde{J}_1 < \tilde{J}_2$, where there is a net attractive interaction and so the phase separation may occur. In the middle region near $j_h/(j_h + U) = 0.5$, a cancellation of \tilde{J}_1 and \tilde{J}_2 leads to a very small net interaction so that the non-uniform charge phase can not be formed. Thus, the phase diagram shown in Fig. 2 is determined by two types of competitions: one competition between hybridization and interaction and the other between the repulsive and attractive interactions, respectively, arising from virtual processes (a) and (b).

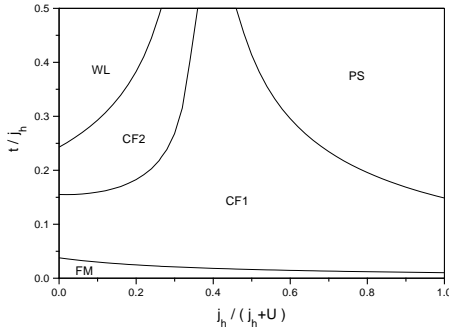


FIG. 2. Phase diagram of t/j_h and j_h/U . The AF coupling constant is taken to be $j_{af}/t = 0.03$. PS stands for the phase separation.

At this stage, we wish to point out that in realistic manganites, the charge ordering is likely to be accompanied by the orbital ordering and the lattice distortion,⁸ which is not considered in the present model, for the main purpose of this work is to examine the effects of the finite J_H and U . More virtual processes will be involved if the orbital degeneracy is taken into account, since there are more mediate states. Meanwhile the lattice distortion will affect the virtual processes due to its effect on the electron hopping. These additional virtual processes may be important in the realistic manganites.

Finally, the present method is not confined to the half-doping case. Fig. 3 is the phase diagram for arbitrary doping, in which, for simplicity, U is set to zero to maximize the effect of process (b). In this case, it is found that the phase separation occurs at either high or low concentrations of the e_g electrons. The phase diagram obtained here is very similar to the result of Monte Carlo simulations.²¹ Similar results were also obtained analytically by other authors^{15,29}. As U is increased, process (b) will be suppressed, since the energy paid necessarily for the double occupancy, $U + J_H S$, will become high. The phase separation disappears when U is large enough. In

doped manganites, the on-site Coulomb interaction U is usually much stronger than the Hund's coupling $J_H S$. However, if the orbital degeneracy at each site is further taken into account, the energy paid for the doubly occupancy might be much lower than $U + J_H S$, for two e_g electrons at the same site can occupy two different orbits and so their spins can be parallel to each other as well as the core spin. In this sense, the virtual process of the double occupancy may revive. It is worth mentioning that the coincidence of our result at $U = 0$ with the numerical simulation indicates the reliability of our method in this system.

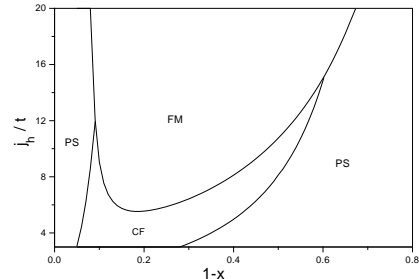


FIG. 3. Phase diagram for $j_{af}/t = 0.01$ and $U = 0$.

V. CONCLUSION

In summary, we have studied an extended Kondo lattice model in the presence of strong but finite Hund's coupling and on-site Coulomb interaction. By means of the Schwinger-boson representation and a mean-field approximation, we show that the effects of the finite J_H and U favor antiferromagnetism. In the half-doping case, it is found that the charge ordering may be superimposed on the magnetic ordering by the repulsive interaction between electrons due to the virtual process of electron hopping. If the on-site Coulomb interaction is weak, the phase separation may occur in either high- or low-doping case. The calculated results show that the finite J_H and U effects play an important role in forming the magnetic ordering and non-uniform charge distributions in the doped manganese oxides.

ACKNOWLEDGMENTS

This work was supported by a CRGC grant at the University of Hong Kong. One of us (D.Y.X) acknowledges support from the National Natural Science Foundation of China.

-
- ¹ R.von Helmolt, et al., Phys. Rev. Lett. **71**, 2331 (1993).
- ² S. Jin, et al., Science **264**, 413 (1994); M. McCormack et al., Appl. Phys. Lett. **64**, 3045 (1994).
- ³ Y. Tokura et al., J. Phys. Soc. Jpn. **63**, 3931 (1994); A. Asamitsu et al., Nature (London) **373**, 407 (1995).
- ⁴ J. Fontcuberta et al., Phys. Rev. Lett. **76**, 1122 (1996).
- ⁵ C. Zener, Phys. Rev. **82**, 403 (1951).
- ⁶ P. W. Anderson and H. Hasegawa, Phys. Rev. **100**, 675 (1955).
- ⁷ P. G. de Gennes, Phys. Rev. **118**, 141 (1960).
- ⁸ J. B. Goodenough, Phys. Rev. **100**, 564 (1955); K. Kubo and N. Ohata, J. Phys. Soc. Jpn. **33**, 21 (1972).
- ⁹ H. Kuwahara et al., Science **270**, 961 (1995); T. Vogt et al., Phys. Rev. B **54**, 15303 (1996).
- ¹⁰ Y. Tomioka et al., Phys. Rev. Lett. **74**, 5108 (1995).
- ¹¹ J. Inoue and S. Maekawa, Phys. Rev. Lett. **74**, 3407 (1995); M. Yamanaka, W. Koshibae and S. Maekawa, Phys. Rev. Lett. **81**, 5604 (1998).
- ¹² R. Shiina, T. Nishitani and H. Shiba, J. Phys. Soc. Jpn. **66**, 3159 (1997).
- ¹³ S. Ishihara, M. Yamanaka, and N. Nagaosa, Phys. Rev. B **56**, 686 (1997).
- ¹⁴ J. van den Brink and S. Khomskii, Phys. Rev. Lett. **82**, 1016 (1999).
- ¹⁵ D. P. Arovas and F. Guinea, Phys. Rev. B **58**, 9150 (1998).
- ¹⁶ A. J. Millis, P. B. Littlewood, and B. I. Shraiman, Phys. Rev. Lett. **74**, 5144 (1995); A. J. Millis, B. I. Shraiman, and R. Mueller, *ibid.* **77**, 175 (1996).
- ¹⁷ A. S. Alexandrov and A. M. Bratkovsky, Phys. Rev. Lett. **82**, 141 (1999).
- ¹⁸ T. T. M. Palstra et al., Phys. Rev. B **56**, 5104 (1997).
- ¹⁹ L. Sheng et al., Phys. Rev. Lett. **79**, 1710 (1997); E. Müller-Hartmann and E. Dagotto, Phys. Rev. B **54**, R6819 (1996); C. M. Varma, Phys. Rev. B **54**, 7328 (1996), D. Y. Xing, S. J. Xiong and D. Feng, Phys. Rev. B **58**, 14139 (1998).
- ²⁰ F. Zhong, J. Dong and Z. D. Wang, Phys. Rev. B **58**, 15310 (1998).
- ²¹ S. Yunoki et al., Phys. Rev. Lett. **80**, 845 (1998); E. Dagotto et al., Phys. Rev. B **58**, 6414 (1998); A. Moreo, S. Yunoki and E. Dagotto, Science **283**, 2034 (1999) and references therein.
- ²² S. Q. Shen and Z. D. Wang, Phys. Rev. B **58**, R8877 (1998).
- ²³ S. Q. Shen, Phys. Lett. A **235**, 403 (1997); S. Q. Shen and Z. D. Wang, Phys. Rev. B (to be published).
- ²⁴ A. J. Millis, Nature **392**, 438 (1998).
- ²⁵ See A. Auerbach, *Interacting Electrons and Quantum Magnetism* (Springer-Verlag, Berlin, 1994)
- ²⁶ S. K. Sarker, J. Phys.: Condens. Matter **8**, L515 (1996).
- ²⁷ S. K. Mishra, R. Pandit, and S. Satpathy, Phys. Rev. B **56**, 2316 (1997).
- ²⁸ J. D. Lee and B. I. Min, Phys. Rev. B **55**, R14713 (1997); L. Sheng and C. S. Ting, Phys. Rev. B **57**, 5265 (1998).
- ²⁹ E. L. Nagaev, Phys. Rev. B **58**, 2415 (1998).